# CHAPTER – 8

# METAMORPHIC CONDITION

## 8.1 Introduction

An estimate of the *P–T* condition is a challenging exercise for the rocks because they underwent different metamorphism episodes. The mineral compositions are not free from re-equilibration during cooling, which affects the peak composition by cation exchanges. It is established that the mineral compositions in natural rocks are difficult to interpret and expected to get the 'preserve equilibrium distributions' of all elements of concern from peak conditions. This 'difficult-to-quantify' compositional variability affects the precision and accuracy of thermobarometry approaches more seriously than the mineral assemblage (petrogenetic grid) approach.

An attempt has been made to discuss the paragenesis and phase relations of different mineral assemblages of the coexisting mineral phases at varying *P–T* conditions based on the mineral chemistry data, along with bulk composition modelling of the pelitic granulites, garnet-biotite gneisses and amphibolites.

# PART-A: PHASE PETROLOGY

## 8.A.1 Introduction

The study of various mineral parageneses is generally supported by graphical projections in pertinent systems, known as phase diagrams. These chemographic projections provide an easy tool for understanding the phase compatibility relationships and for deducing metamorphic reactions involved in the formation of diverse mineral assemblages. The phase relationship and the analyses of coexisting minerals in a pertinent system will provide the data which indicates equilibrium crystallization or any disappearance from chemical equilibrium.

The reaction textures, which are present as coronas and symplectites, suggest disequilibrium during metamorphic crystallization. Each mineral assemblage would be located at a distinct *P–T* point, indicating metamorphism conditions.

This chapter attempts to discuss the parageneses and phase relations of different mineral assemblages from pelitic granulites, garnet-biotite gneisses, and amphibolites.

### 8.A.2 Phase compatibility relations

#### 8.A.2.1 Pelitic granulites

To begin the discussion in respect of interpreting the quartzofeldspathic and pelitic assemblages in these rocks, AKF projections have been used. For clarity, individual rock types are plotted in separate diagrams (see Fig.8.1).

The mineral assemblages of these rocks have been graphically represented in the AKF diagram. The divariant metamorphic reactions involved in the formation of pelitic granulites can be easily derived from the AKF diagram (Fig.8.1).

The biotite and plagioclase were continuously consumed during the prograde stage to form garnet through the biotite-melting dehydration reaction.

Bt + Sil + Qz → Grt + Kfs + Melt……(1)

Bt + Pl + Qz → Grt + Melt…….(2)

Here, one three-phase field of garnet-biotite-sillimanite and is evident from biotite-sillimanite join intersected by garnet-K-feldspar joins in the AKF diagram (Fig.8.1).

As the pressure began to increase, coarse-grained orthopyroxene started to form adjacent to small garnet relicts reflecting the following reactions;

Grt + Qz → Opx + Pl……(3)

Bt + Pl + Qz → Opx + Grt + Melt……..(4)

When the pressure decreases, matrix cordierite forms in conjunction with matrix biotite, quartz, and plagioclase. Cordierite grains are observed in the vicinity of garnet grains,

indicating a possible reaction texture. The continuous Fe-Mg reactions in the three-phase field of garnet-cordierite-sillimanite are represented in Figure 8.1.

Grt+ Bt + Qz → Crd + Melt……(5)

Grt + Sil + Kfs + Qz → Crd + Bt + Melt…….(6)

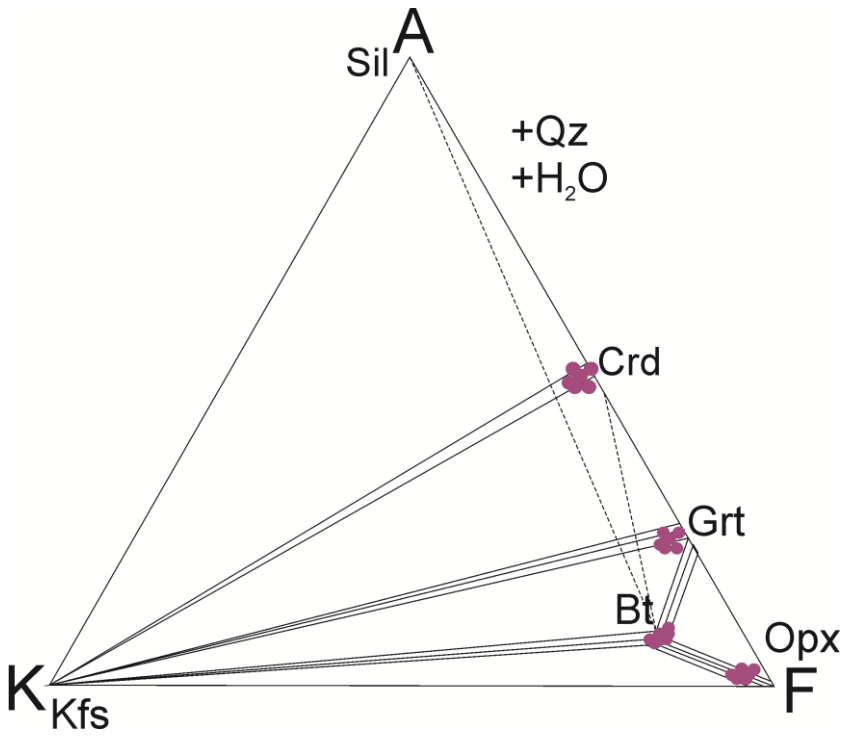


**Figure 8.1** AKF Diagrams, A = ($Al_2O_3$ + $Fe_2O_3$) – ($K_2O$ + $Na_2O$ + CaO); K = $K_2O$; F = FeO + MnO + MgO, (A + K + F = 100 mol%). For the pelitic granulites solid coloured circles correspond to the observed mineral assemblages in the investigated area.

Both (5 and 6) are continuous Fe-Mg reactions. The relative $X_{Mg}$ in the phases concerned here: Crd>Bt>Grt core >Grt rim, the $T_{Mg}$is more than $T_{Fe}$. Thus, both three-phase fields would shift towards the lower $X_{Mg}$ side during cooling and hydration due to the reversal of the reaction (5) and (6). The shift of the three-phase fields towards Fe-rich of the AFM diagram during retrogression or cooling may also be related to changes in pressure conditions due to uplift during this episode.

### 8.A.2.2 Garnet-biotite gneisses

The garnet-biotite gneisses are plotted in the FeO-MgO-$Al_2O_3$-$SiO_2$-$H_2O$ (FMASH) system in the AKF projection diagram (Fig.8.2). The mineral parageneses that result from the

reaction between garnet and biotite reflect the stability of garnet-biotite. The mineral association is a poly-metamorphism product and is an association of mineral assemblages of different metamorphic stages. The following metamorphic reactions support these:

Peak reaction: It contains an inclusion of biotite along with plagioclase and quartz at various places, suggesting the following reaction:

$Bt + Pl + Qz \rightarrow Grt + Kfs + H_2O$……(7)

Post-peak reaction: biotite and quartz border the porphyroblasts of garnet, which provides evidence for late hydration during cooling as the pressure continuously decreases, indicating the following reaction:

$Grt + Pl + H_2O \rightarrow Bt + Qz$……..(8)

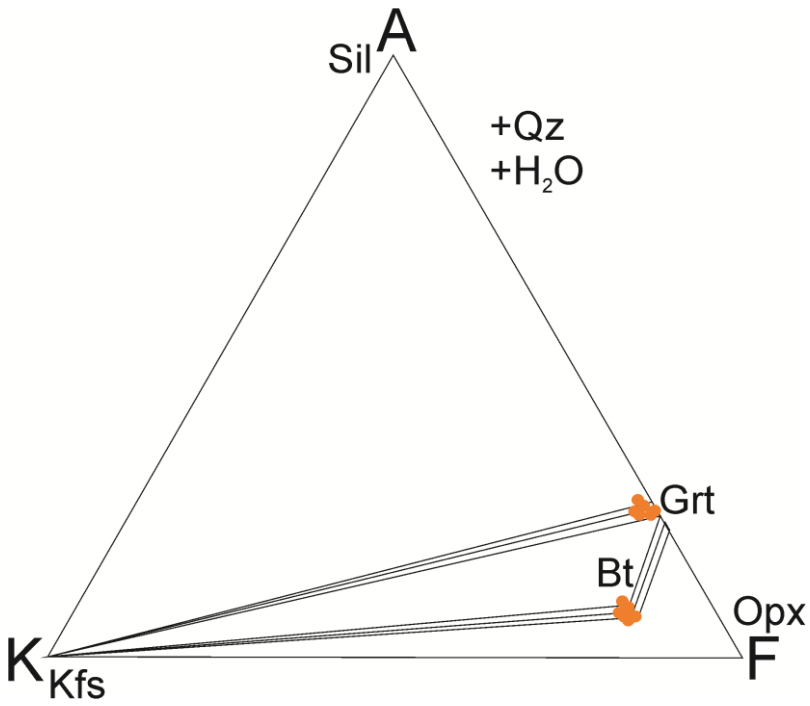


**Figure 8.2** AKF Diagrams, A = ($Al_2O_3$ + $Fe_2O_3$) – ($K_2O$ + $Na_2O$ + CaO); K = $K_2O$; F = FeO + MnO + MgO, (A + K + F = 100 mol%). For the garnet-biotite gneisses solid coloured circles correspond to the observed mineral assemblages in the investigated area.

### 8.A.2.3 Amphibolites

The phase relationships of the garnet-bearing and garnet-absent amphibolites have been discussed in the model system of CaO-(MgO+FeO)-$Al_2O_3$-$SiO_2$-$H_2O$ and first investigated

graphically in the ACF diagram (Fig.8.3a&b), with the components of this subsystem suitably represent the coexisting grt, cpx, hbl, and plg. $Na_2O$ is a significant content of plagioclase and hornblende, whereas FeO and $TiO_2$ are common in hornblende. Biotite and k-feldspar occur as the limited amount may be due to the non-availability of $K_2O$, so $K_2O$ has been neglected for graphical representation. In particular, the garnet-clinopyroxene-plagioclase mineral assemblage (Fig.8.3a) occurs in response to the hornblende break down, forming a three-phase field by breaking the tie lines hornblende-plagioclase, hornblende-clinopyroxene, and hornblende-garnet through the reaction (8). This reaction (8) is a continuous reaction that primarily depends on quartz's availability for the complete breakdown of amphibole. Several metamorphic reactions have been observed in amphibolites, which are described as:

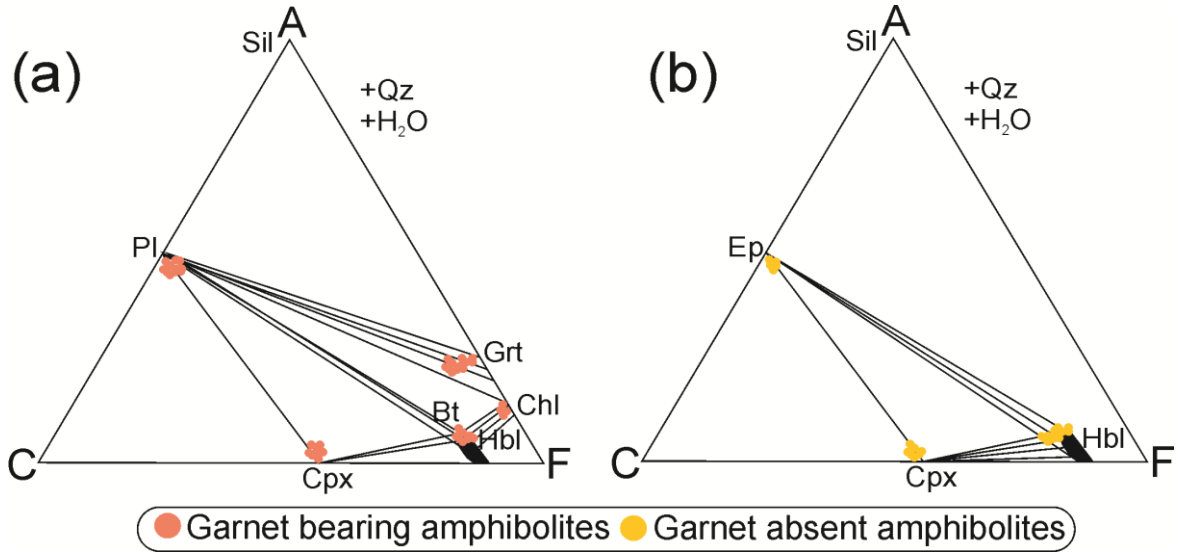


**Figure 8.3** The mineral composition of the amphibolites are shown in ACF diagram where, A = ($Al_2O_3$ + $Fe_2O_3$) – ($K_2O$ + $Na_2O$); C = CaO; F = FeO + MgO + MnO. (A+C+F = 100 mol%), (a) observed mineral assemblages in garnet bearing amphibolites, (b) observed mineral assemblages in garnet absent amphibolites.

The pre-peak metamorphic assemblage has been recognized as Grt-Amp-Chl-Bt-Pl-Ilm-Qz, which contains amphibole, chlorite, biotite, plagioclase, and ilmenite as inclusions inside garnet porphyroblast. These textural features suggest a pre-peak prograde metamorphic condition, with the following reaction:

Chl + Bt + Qz→ Grt + Amp + Melt……..(9)

Amp + Pl → Grt + Qz + Melt……(10)

The following reactions form the peak metamorphic assemblage:

Amp + Qz → Cpx + Grt + Melt…….(11)

Amp + Pl + Qz → Grt + Cpx + Amp + Pl…….(12)

Bt + Qz → Cpx + Amp + Melt…….. (13)

The post-peak metamorphic assemblage is defined by Amp-Bt-Pl-Ilm-Qz. Here, amphibole is present as the majority of the matrix. The following reactions are inferred:

Cpx + Melt → Amp + Bt + Qz……(14)

Cpx + Pl + Melt → Amp + Qz……(15)

Grt + Bt + Melt → Amp + Qz + Melt…….(16)

## PART B- BULK COMPOSITION MODELLING

### 8.B.1 Application of equilibrium thermodynamics

Advances in the understanding of the thermodynamic behaviour of metamorphic phases, both rock-forming and accessory constituents (e.g. Holland and Powell, 1985, 1998; Powell and Holland, 1985; Berman, 1988; Gottschalk, 1996), permit the calculation of average conditions of crystallization and quantitative phase diagrams for mineral systems thought to record chemical equilibrium. This method is useful for determining the *P*–*T* pathways of exhumed metamorphic rocks. To calculate geologically accurate P–T–X relations from metamorphic rocks, it is critical that the system's (i.e., mineral assemblage or sub–assemblage) phases are shown to represent a state of thermodynamic equilibrium.

Given that metamorphism is a dynamic process, with P, T, and X changing throughout a metamorphic rock's evolution, it is uncertain whether the chemical equilibrium is a valid assumption. The kinetics of intergranular diffusion exerts a dominant control on the time and length scales of metamorphic equilibration (Carlson, 2002). Quantitative knowledge of intergranular diffusion rates for major and trace elements remains unknown. However, an

intergranular fluid phase promotes higher rates of elemental exchange and, hence, metamorphic equilibration (Carlson, 2011). Accordingly, prograde (dehydration) metamorphic reactions proceed more rapidly than retrograde (hydration) reactions—accounting for the common preservation of mineral assemblages formed under peak T conditions. This is supported by confirming predictions from phase equilibria modelling and observed metamorphic mineral assemblages. Despite the theoretical validation of the equilibrium condition, commonly observed coronal microstructures (Ashworth and Birdi, 1990; Johnson and Carlson, 1990), linked segregations (Carmichael, 1969), and pseudomorphous growth structures (Foster Jr., 1986) provide petrographic evidence for chemical disequilibrium, where reactions cease before the total consumption of reactants. Such evidence is commonly found in $H_2O$ under under-saturated conditions and suggests sluggish intergranular diffusion kinetics. Accordingly, it is fundamentally essential to screen samples for petrographic evidence of disequilibrium before applying equilibrium thermodynamic principles. The equilibrium model of metamorphism cannot be "proved" in the same way as disequilibrium; instead, the absence of disequilibrium features is generally taken as supporting evidence. Furthermore, equilibrium assemblages must obey the phase rule ($F = C + 2 - P$, where F = variance, C = number of components, and P = number of phases present) and show consistent element partitioning between co-genetic phases.

Accepting the valid application of equilibrium thermodynamics to metamorphic rocks, thermodynamic descriptions of relevant phases (e.g., Helgeson et al., 1978) are combined with activity–composition models (a–x) describing the energetics of end-member phase interaction, to permit calculation of the assemblage's peak *P*–*T*. Initially, this approach was limited to precisely calibrated reactions (e.g., Ferry and Spear, 1978), followed by consideration of numerous reactions, which allowed the calculation of average *P*–*T* conditions (Powell, 1985; Powell and Holland, 1988, 1994). However, such thermobarometry is limited by a dependence on mineral chemistry—inherent to the method's inverse nature. Improvements in the quality and

breadth of thermodynamic data and a–x relations based on the same phase end-member compositions (internally consistent datasets – Holland and Powell, 1990, 1998; Powell and Holland, 1988) underpinned the development of forwarding phase equilibria modelling, i.e., given a reactive composition, *P–T*, *P–X*, or *T–X* relations (pseudosections) can be calculated for all phases in the system of interest.

**8.B.2 Pseudosection modelling**

Pseudosection modelling is the most powerful technique for extracting *P–T* data from exhumed metamorphic rocks (e.g. Powell et al., 1998; Tinkham et al., 2001; Powell and Holland, 2010). Pseudosections arose from the construction of petrogenetic grids, which show all the invariant points and univariant lines for all phases and bulk composition in a chemical system (e.g.Hess, 1969; Powell and Holland, 1990). Such grids provide information regarding the absolute stability of assemblages. However, they do not provide information regarding the composition and abundance of phases. Pseudosections offer a means by which the system's petrogenetic grid is modified for a specific bulk composition—effectively forming a mineral assemblage map in P–T–X space (Powell et al., 1998).

The validity of the pseudosection approach relies on an accurate determination of the reactive bulk composition. As discussed above, the length scales of diffusive equilibration are poorly constrained in metamorphic rocks, making this the most significant source of uncertainty inherent to the technique. Rocks containing zoned porphyroblasts are particularly challenging to model as the effective bulk composition changes with porphyroblast growth, meaning that pseudosection topology will vary as a function of time. This effect is typified by garnet's growth, which preferentially sequesters Mn during early growth stages (Mahar et al., 1997). It is possible to mitigate against reactive volume fractionation by selecting a suitable composition of garnet—i.e., from the core (initiation of growth) to rim (cessation of growth) portions—to calculate the

bulk composition. Pseudosections presented in this chapter are based on bulk compositions calculated from combining mineral modes unless otherwise stated.

### 8.B.3 Methodology

The phase diagram has been calculated using the Perple_X 6.9.0 program, which includes various sub-programs. The pseudosection is a diagram showing the various reaction conditions in the *P–T* space, adapted to a particular bulk composition. The effective bulk rock compositions for the pseudosection calculations were obtained from the whole-rock XRF analysis performed at the Birbal Sahni Institute of Palaeosciences (BSIP), Lucknow, India. First, the build program has to be run containing computational option files, and then the Vertex has to be run in which the phase diagram is calculated. Details of solution models are given in the "Perple_X solution model glossary" and "Perple_X Updates" (http://www.perplex.ethz.ch/perplex_updates.html). After this, the Pssect program is run. It usually takes a long time to generate a postscript plot. The crude diagrams are to be finalized in any other graphic editor software. For the generation of the isopleths, the Pywerami program is employed.

### 8.B.4 *P–T* Pseudosections

#### 8.B.4.1 Pelitic granulites

**(i) Grt-Opx-Crd pelitic granulites**

Pseudosection of the representative pelitic granulites sample (M-9) was derived with the help of Perple_X ver.6.9.0 software (Connolly 2005, 2009) and the end-member thermodynamic dataset of Holland and Powell (1998, 2011). For the pelitic granulite, *P–T* pseudosections were calculated in the chemical system $Na_2O$-CaO-$K_2O$-FeO-MgO-$Al_2O_3$-$SiO_2$-$H_2O$-$TiO_2$-$O_2$ (NCKFMASHTO), which is reasonably compatible for modelling the rock examined. The phases that are used in the modelling are orthopyroxene (Holland and Powell, 2003), garnet (Holland and Powell, 2003), melt (Holland and Powell, 2003), cordierite (White et

al., 2014), biotite (Tajcmanova et al., 2009), plagioclase (Fuhrman and Lindsley, 1988), and ilmenite (White et al., 2000). Magnetite, quartz, and aluminosilicates are considered pure phases. For the major element chemical analysis, the same slabs of the examined granulites were used, which were previously used for thin-section preparation.

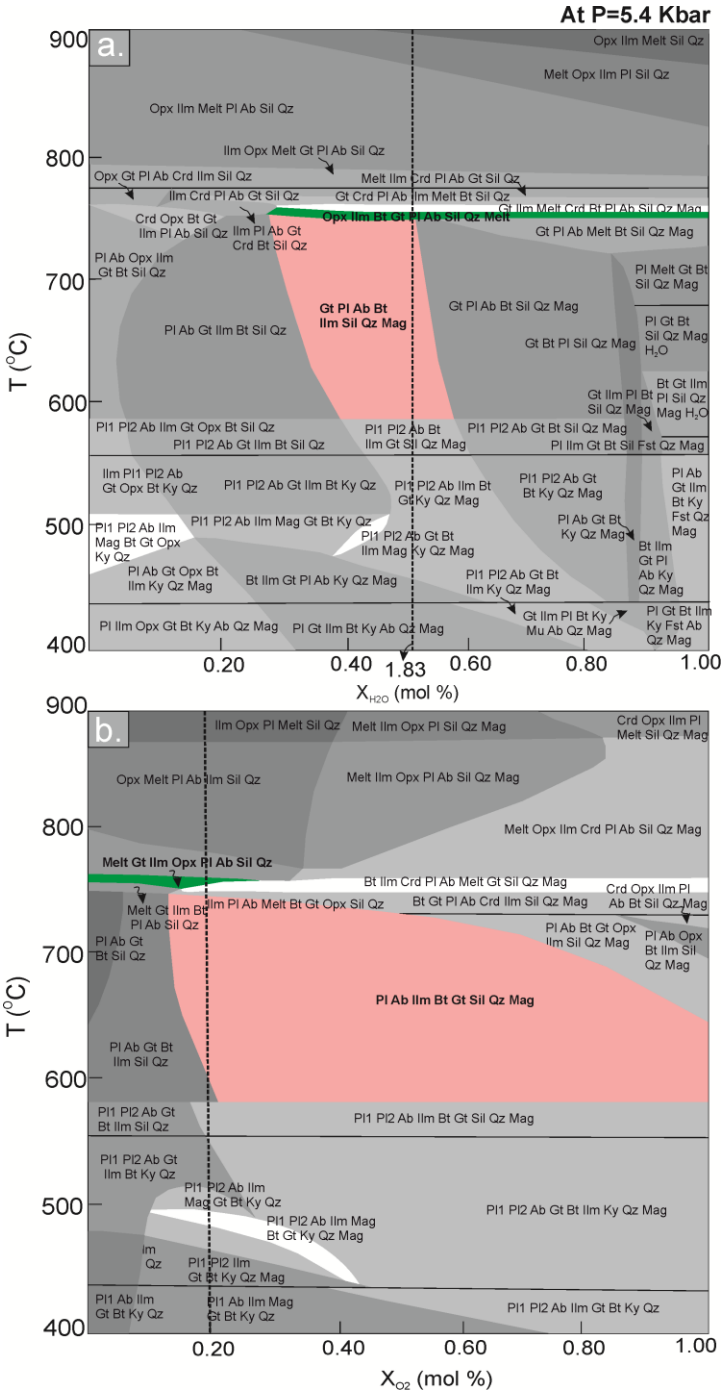


**Figure 8.4** (a) P-X($H_2O$) and (b) P-X($O_2$)diagrams showing calculated pseudosection of mineral assemblages in pelitic granulite (sample M-9) at 5.4 kbar.

The bulk composition of pelitic granulite (M-9) was measured by XRF analysis in weight percentage and then converted into a mole percentage for calculating pseudosections. The sample M-9 composes; $SiO_2$=64.10, $TiO_2$=0.72, $Al_2O_3$=14.25, FeO=9.78, MgO=4.49, CaO=1.46, $Na_2O$=1.03, $K_2O$=2.19, $H_2O$=1.83 and $O_2$ =0.20 (in mol%). The observed mineral assemblage in the sample M-9 (pelitic granulite) involves Grt-Opx-Crd-Bt-Sil-Pl-Kfs-Qz-Ilm ± inferred melt. Figures 8.4a&b show the P-X($H_2O$) and P-X($O_2$) pseudosections of sample M-9 that have been constructed at 5.4 kbar for estimating the probable water content and $O_2$ content of the rock. The observed results suggest that the assemblage is stable up to X($H_2O$)= 1.83 mol% and upto X($O_2$)= 0.20 mol%.

The *P–T* pseudosection has been constructed for the same sample (M-9) in the range of 3–8 kbar and 400–1000ºC (Fig.8.5a). The biotite, sillimanite, and plagioclase define the pre-peak metamorphic condition. Quartz crystals that occur as inclusions within garnet and their respective mineral assemblages are found under low temperature and pressure conditions. The *P–T* condition of pre-peak metamorphism is found in the range of 4.00–5.12 kbar and 560–600°C. The *P–T* condition of this stage is determined from garnet and biotite $X_{Mg}$isopleth contour lines that are identical to the studied microprobe data. The peak assemblage (grt + opx + bt + plg + sill + kfs + melt + ilm + qz) has a *P–T* stability field ranging from 6.40–6.62 kbar and 700–730°C. The contouring of the $X_{Mg}$ isopleth line of garnet and orthopyroxene yielded this peak metamorphic state (Fig.8.5b). The petrographic examination has revealed the isothermal decompression retrograde reaction, in which the consumption of garnet results in the creation of cordierite under low-pressure circumstances, implying the following reaction: Crd + bt + kfs + melt Grt + sill + qz. At higher pressures, garnet, biotite, and sillimanite bearing assemblages are stable, whereas cordierite bearing assemblages dominate in the pseudosection's low-pressure equilibrium field. Cordierite is found in the matrix during the retrograde metamorphic stage, with lower $X_{Mg}$ values. The retrograde metamorphic assemblage in *P–T* pseudosection contains

grt + crd + bt + plg + kfs + melt + ilm + qz, which are stable in the range of 4.20–4.40 kbar pressure and 670–692°C temperature according to the textural interpretation.

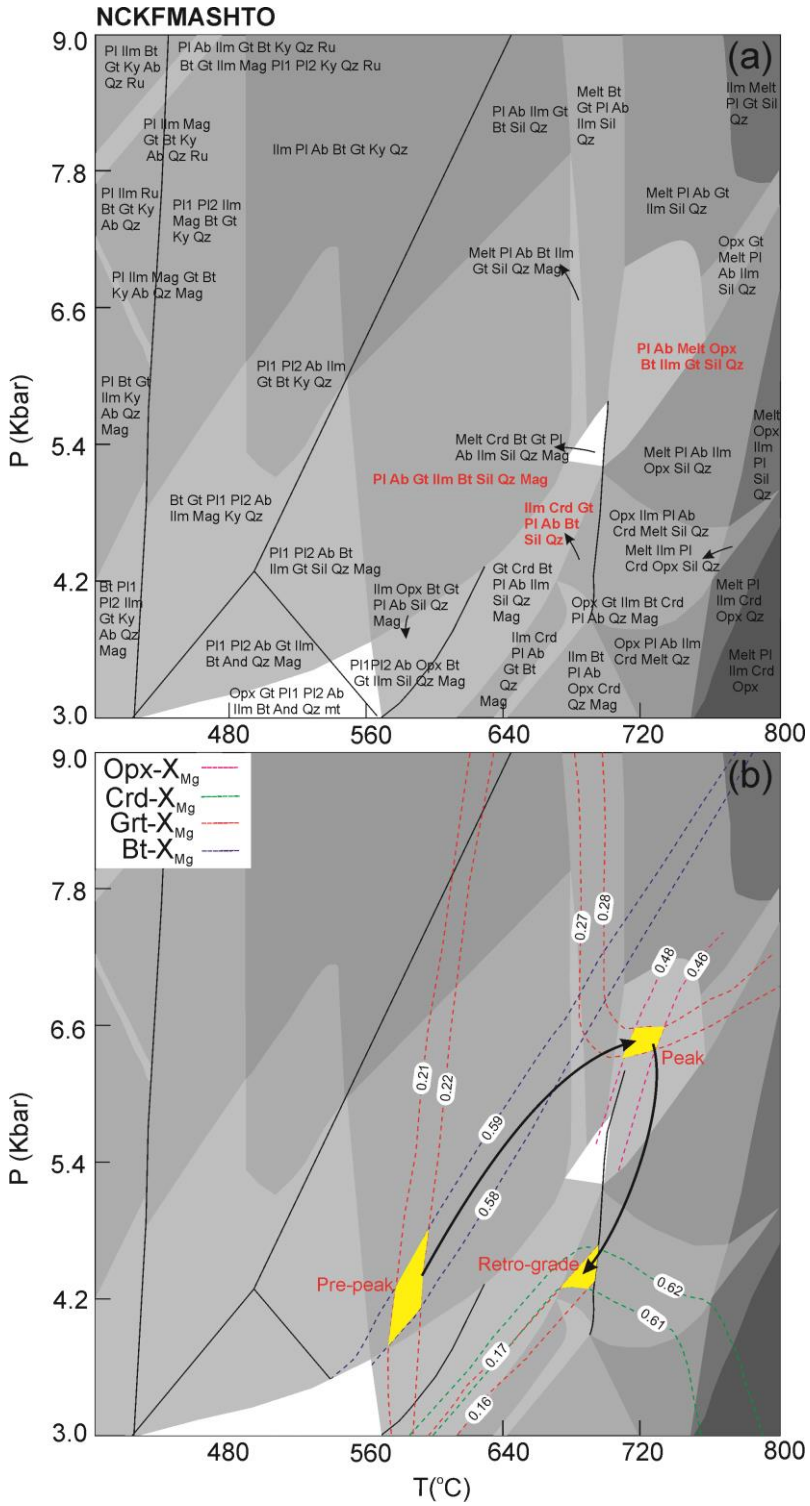


**Figure 8.5** *P-T* pseudosection of mineral assemblage in pelitic granulite (sample M-9) in the NCKFMASTHO system, (b) contouring isopleths ($X_{Mg}$) of garnet, orthopyroxene, cordierite and biotite.

**(ii) Grt-Opx-Bt pelitic granulites**

Pseudosection of the representative pelitic granulites sample (PM2) was derived with the help of Perple_X ver.6.9.0 software (Connolly 2005, 2009) and the end-member thermodynamic dataset of Holland and Powell (1998, 2011). For the pelitic granulite, *P–T* pseudosections were calculated in the chemical system $Na_2O$-CaO-$K_2O$-FeO-MgO-$Al_2O_3$-$SiO_2$-$H_2O$-$TiO_2$-$O_2$ (NCKFMASHTO), which is reasonably compatible for modelling the rock examined. The phases that are used in the modelling are orthopyroxene (Holland and Powell, 2003), garnet, melt (White et al., 2014), biotite (Tajcmanova et al., 2009), plagioclase (Fuhrman and Lindsley, 1988), ilmenite (White et al., 2000). Magnetite, quartz, and aluminosilicates are considered pure phases. For the major element chemical analysis, the same slabs of the examined granulites were used, which were previously used for thin-section preparation. The measured whole-rock composition of PM2 (pelitic granulite) was normalised in mol%, and they are: $SiO_2$=63.34, $TiO_2$=0.80, $Al_2O_3$=12.62, FeO= 9.81, MgO= 5.25, CaO= 2.26, $Na_2O$= 1.31, $K_2O$= 2.58, $H_2O$=1.83 and $O_2$ =0.20 (in mol%). MnO content is low and hence neglected in pseudosection construction. Quartz is taken in excess as it is ubiquitous in all assemblages observed in pseudosection.

The observed mineral assemblage in the sample PM2 (pelitic granulite) involves Grt-Opx-Bt-Sil-Pl-Kfs-Qz-Ilm±inferred melt, representing the peak metamorphism. Figures 8.6a&b show the P-X($H_2O$) and P-X($O_2$) pseudosections of sample PM2 that have been constructed at 850°C for estimating the probable water content and $O_2$ content of the rock. The observed results suggest that the assemblage is stable up to X($H_2O$)= 0.6 mol% as k-feldspar disappears at X($H_2O$) >0.6mol%. Similarly, the P-X($O_2$) pseudosection reveals that the assemblage is stable up to X($O_2$)= 0.6 mol%.

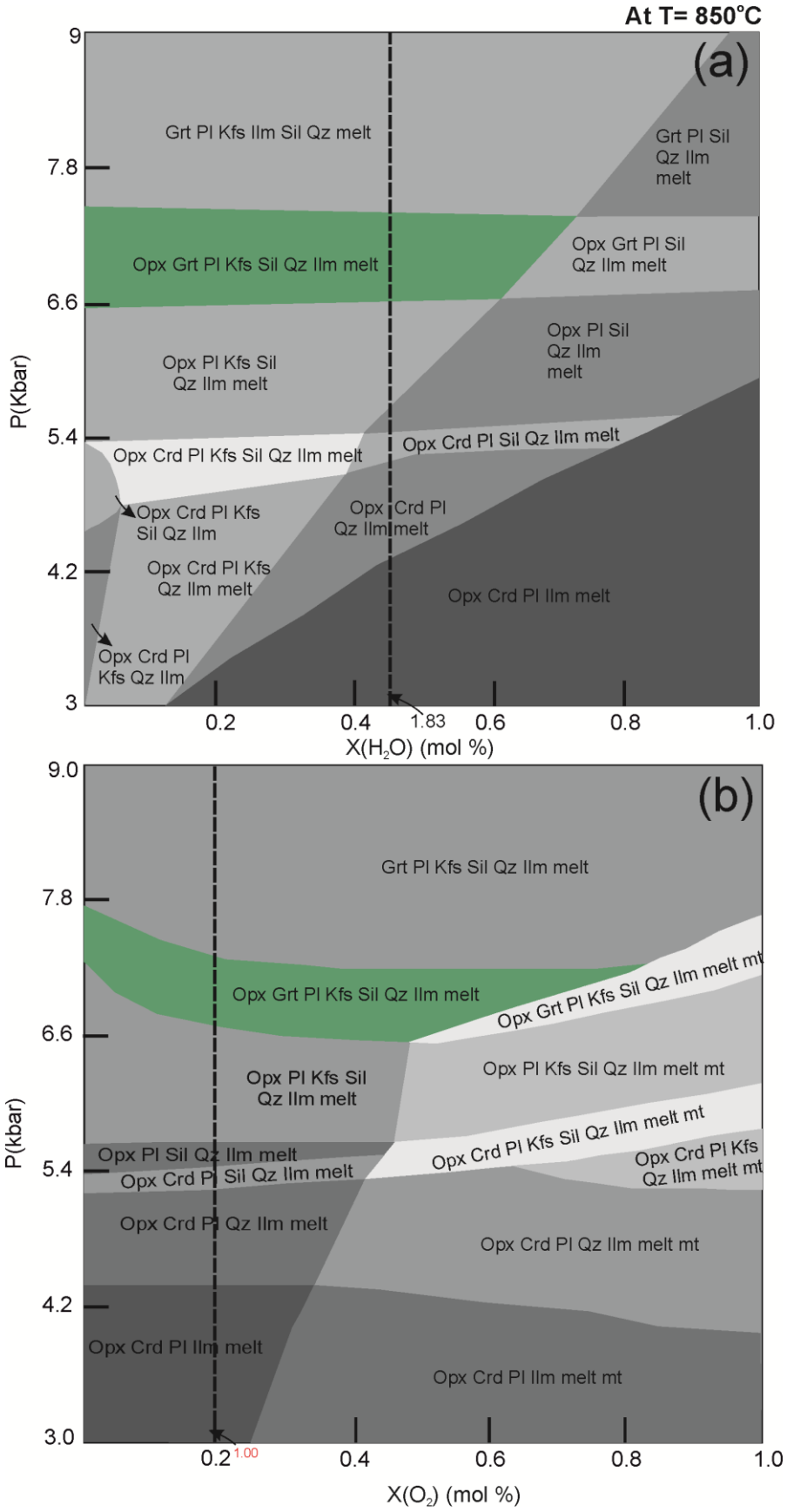


**Figure 8.6** (a) P-X($H_2O$) and (b) P-X($O_2$)diagrams showing calculated pseudosection of mineral assemblages in pelitic granulite (sample PM-2) at 850ºC.

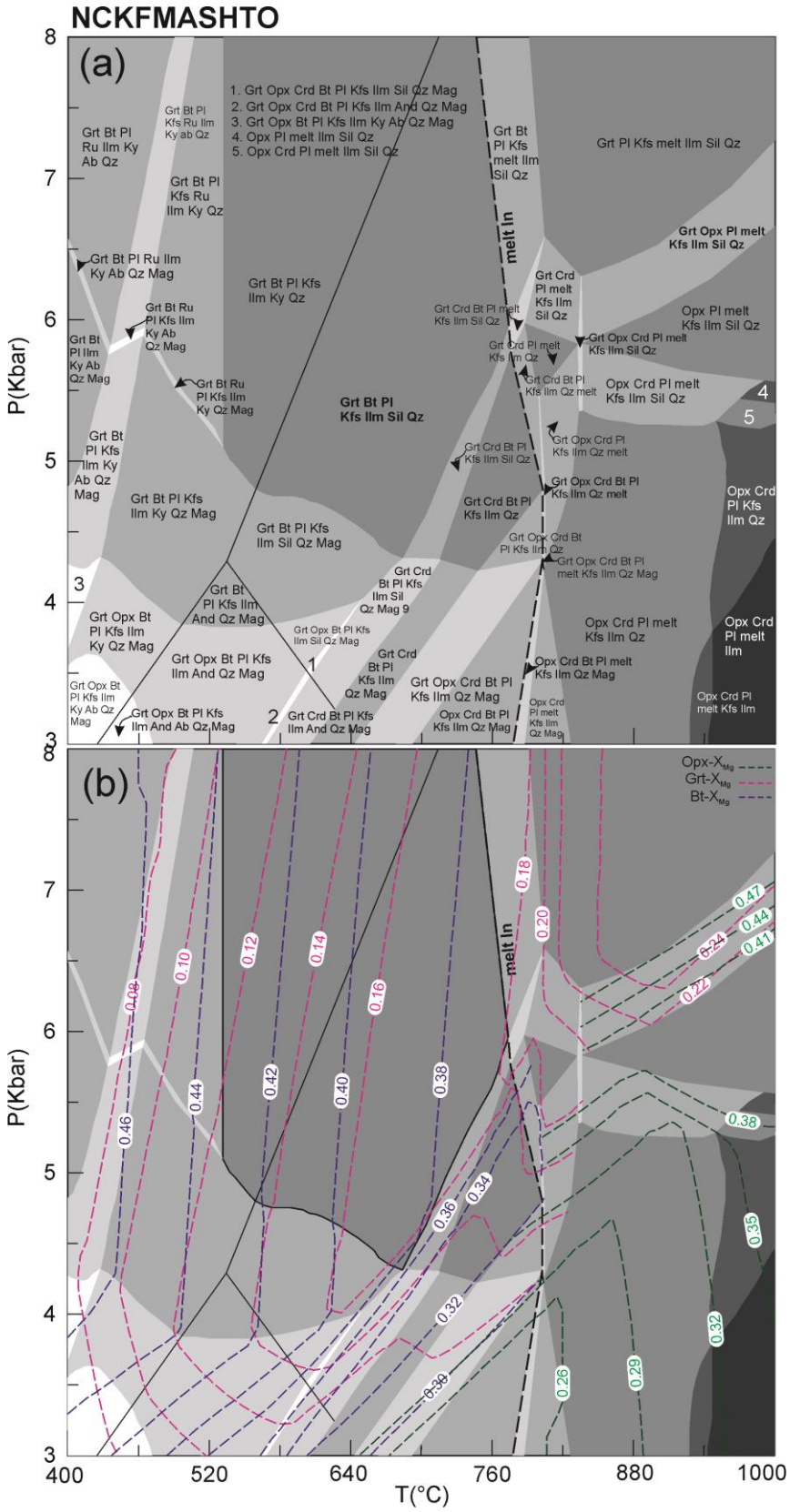


**Figure 8.7** *P-T* pseudosection of mineral assemblage in pelitic granulite (sample PM-2) in the NCKFMASTHO system, (b) contouring isopleths ($X_{Mg}$) of garnet, orthopyroxene and biotite.

The *P–T* pseudosection has been constructed for the same sample (PM2) in the range of 3–8 kbar and 400–1000ºC, and the constructed diagram is represented in Figure 8.7a. The calculated pseudosection for the pelitic granulite is admissible to the mineral assemblages observed in petrography. The progressive mineral phase of the rock is demarcated by the presence of garnet, sillimanite, plagioclase, and biotite mineral assemblages with a *P–T* range of > 4.3 kbar and 540ºC to 750ºC. The upper-temperature stability limit of the assemblage is defined by the presence of melt, whereas the lower limit is defined by the presence of magnetite. However, biotite and quartz react to form the garnet and orthopyroxene at a higher temperature, representing the peak mineral assemblage (garnet, orthopyroxene, sillimanite, plagioclase, k-feldspar, ilmenite, quartz, and melt). The *P–T* window of peak mineral assemblage ranges from 5.8 kbar to 7.2 kbar and >825ºC. Biotite is stable up to 790°C temperature, and plagioclase is stable throughout the phases. Orthopyroxene is stable at low-pressure conditions and shows a proportional relationship between temperature and pressure conditions. In contrast, garnet shows a disproportionate relationship, which means that garnet disappears as temperature increases and is stable only at high pressure. The pseudosection is also contoured with the isopleths of $X_{Mg}$ garnet, $X_{Mg}$ orthopyroxene, and $X_{Mg}$ biotite (Fig.8.7b). Garnet and orthopyroxene isopleths show steep slopes with $X_{Mg}$ content continuously increasing with increasing temperature, whereas the $X_{Mg}$ content of biotite constantly decreases with increasing temperature.

**(iii) Grt-Bt-Sill pelitic granulites**

Pseudosection of the representative sample (K-2) was modelled in the $Na_2O$-CaO-$K_2O$-FeO-MgO-$Al_2O_3$-$SiO_2$-$H_2O$-$TiO_2$-$O_2$ (NCKFMASHTO) system, using Perple_X ver.6.9.0 software (Connolly 2005, 2009) and the end-member thermodynamic dataset of Holland and Powell (1998, 2011) (Fig. 8.8). Garnet, biotite, sillimanite, and plagioclase are the minerals' dynamic data sets selected for the construction of pseudosection. Different solid solution models used are garnet, melt (Holland and Powell, 1998); biotite (Tajcmanova et al., 2009); ilmenite

(White et al., 2000); and plagioclase (Fuhrman and Lindsley, 1988). Then the quartz, magnetite, and aluminosilicates are taken as pure end members.

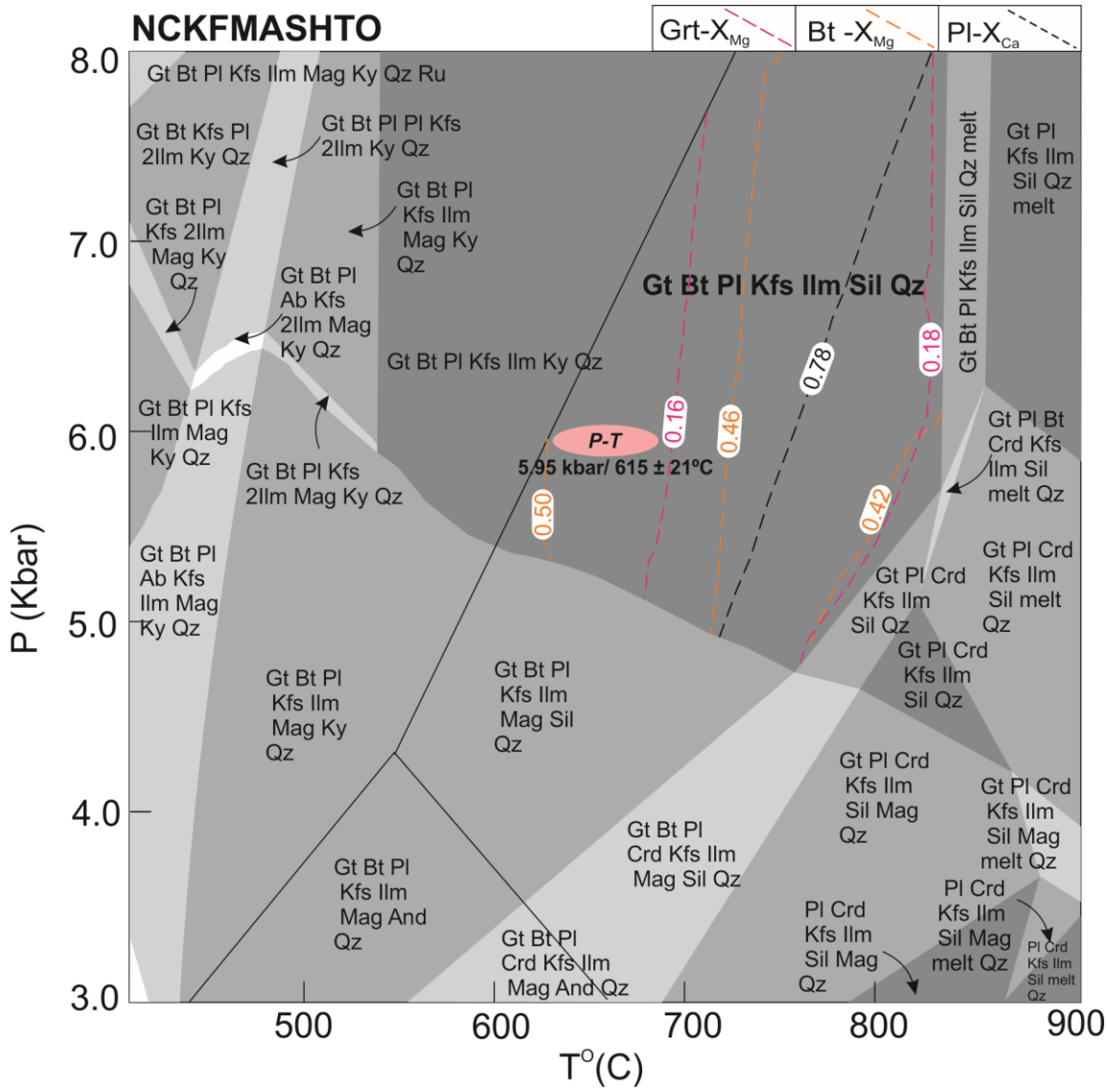


**Figure 8.8** Pseudosetion of representative sample showing different mineral assemblages at different *P-T* conditions along with isopleths of garnet, biotite and plagioclase.

The *P–T* pseudosection is constructed in the range of 3–8 kbar and 400–900ºC. The measured bulk composition of the modeled sample (K-2) in mol% is $SiO_2$ = 72.52, $Al_2O_3$ = 12.29, CaO = 1.56, FeO = 6.89, $K_2O$ = 1.29, MgO = 2.45, $Na_2O$ = 1.34, $TiO_2$ = 0.69, $H_2O$ = 0.75, $O_2$ = 0.20. MnO content is low and hence neglected in pseudosection construction. Quartz is taken in excess as it is ubiquitous in all assemblages observed in pseudosection. The $O_2$ has been estimated by integrating mineral compositions and modal abundance data of the phases

presented in the rock. The $H_2O$ is present in hydrous mineral phases like biotite, in which ~5-6 wt% $H_2O$ constitutes about 15% of the total rock volume. This observation suggests ~0.75 mol% $H_2O$ for the bulk rock composition. The calculated pseudosection is relevant to the mineral assemblages observed in petrography. The observed mineral assemblage, Grt-Bt-Pl-Kfs-Sill-Ilm-Qz, is stable in the *P–T* range of 570-820ºC and 5.5–8.0 kbar. It is necessary to constrain the *P–T* values of the assemblage further to get the approximate values of the *P–T* condition for the sample. Hence, the pseudosection is also contoured with the isopleths of $X_{Mg}$ garnet, $X_{Mg}$ biotite, and $X_{Ca}$ plagioclase. The isopleths further narrow down the *P–T* condition values to 5.95 kbar/615±21 ºC.

**8.B.4.2 Garnet-biotite gneisses**

**(i) Sample M1-A1**

Metamorphic *P–T* conditions of the garnet-biotite-plagioclase-k-feldspar-melt-ilmenite-quartz stable mineral assemblage have been constrained using the Perple_X ver.6.9.0 software (Connolly, 2005, 2009), and end-member thermodynamic data were taken from Holland and Powell (2011). The pseudosection of the representative sample (M1-A1) has been prepared in the NCKFMASHT system ($Na_2O$-CaO-$K_2O$-FeO-MgO-$Al_2O_3$-$SiO_2$-$H_2O$-$TiO_2$). The solid solution models for various minerals have been considered in this phase of equilibrium modelling, such as; garnet, melt (W: White*et al.*, 2014), plagioclase (HP: Holland and Powell, 2003), feldspar (feldspar: Fuhrman and Lindsley, 1988), biotite (TCC: Tajcmanová *et al.*, 2009), and ilmenite (WPH: White *et al.*, 2000). Alumino-silicates, quartz, and magnetite are treated as pure end-member phases. The measured bulk compositions of the modeled sample (M1-A1) in mol% are: $SiO_2$ = 61.77, $Al_2O_3$ = 10.19, CaO = 2.12, FeO = 9.12, $K_2O$ = 2.09, MgO = 8.07, $Na_2O$ = 2.11, $TiO_2$ = 1.04 and $H_2O$ = 3.50. MnO and $P_2O_5$ contents are very low; hence it is neglected in pseudosection construction, whereas $P_2O_5$ is used in the recalculation of CaO.

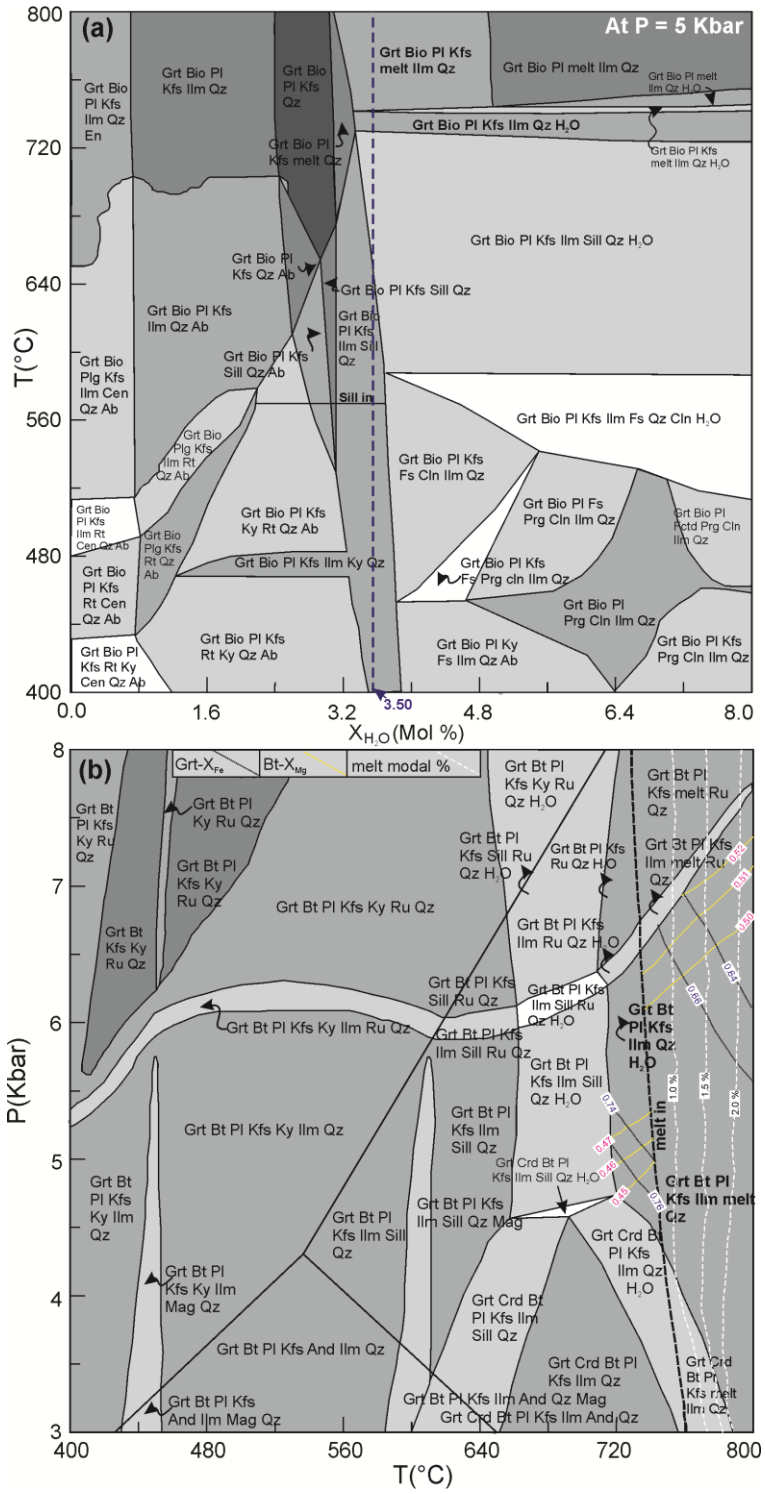


**Figure 8.9** (a) T–$X_{H2O}$pseudosection at 5.0 kbar, showing the effects of varying the molar proportions of bulk-rock $H_2O$, black dash line is modelled composition of $H_2O$ (3.50 %). (b) pseudosetion (M1-A1) is calculated in NCKFMASHT system, and Isopleth lines for garnet ($X_{Mg}$), biotite ($X_{Mg}$), and melt modal %.

Grt-Bt gneisses contain bands of leucosome as a sign of the availability of melt. Melt is an essential constituent of any metamorphic rock, so it is considered in phase equilibria

modelling. Here, the amount of $H_2O$ is constrained with the help of the T-$X_{H2O}$ pseudosection (Fig.8.9a), and it is constructed at 5.0 kbar pressure. The molar composition of $H_2O$ is plotted along the X-axis in the T-X($H_2O$) pseudosection. The computed amount of $H_2O$ varies from the anhydrous composition ($X_{H2O}$ = 0 mol %) to excess $H_2O$ ($X_{H2O}$ = 8.0 mol %). The X($H_2O$) value of 3.50 mol% is an appropriate constituent for forming stable mineral assemblages (Grt-Bt-Pl-Kfs-melt-Ilm-Qz).

The *P–T* pseudosection is constructed in the range of 3–8 kbar and 400–800ºC (Fig. 8.9b). Garnet, biotite, and quartz are ubiquitous in the *P–T* pseudosection. The required mineral assemblage (Grt-Bt-Pl-Kfs-melt-Ilm-Qz) represented a peak metamorphic assemblage and occupied a field in the *P–T* range of 6.35–6.75 kbar and 755–780ºC. The *P–T* condition is calibrated with the help of isopleth lines of $X_{Mg}$ garnet and $X_{Mg}$ biotite. The calculated pseudosection is admissible for mineral assemblages observed in petrography. Instead of this, we have also observed similar mineral assemblages under lower pressure and temperature conditions. The melt phase does not exist here, whereas $H_2O$ is available as a component. Therefore, we would like to say that this stable phase may evolve during the retrograde metamorphic condition. Their *P–T* condition is comparatively low, between 4.80–5.28 kbar and 718–735ºC.

**(ii) Sample M-1A**

Pseudosection of the representative Grt- Bt gneiss sample (M-1A) were derived with the help of Perple_X ver.6.9.0 software (Connolly 2005, 2009) and end-member thermodynamic dataset Holland and Powell (1998, 2011). For the Grt-Bt gneiss, *P–T* pseudosections were calculated in the chemical system $Na_2O$-CaO-$K_2O$-FeO-MgO-$Al_2O_3$-$SiO_2$-$H_2O$-$TiO_2$ (NCKFMASHT), which is reasonably compatible for modelling the rock examined. The phases that are used in the modelling are orthopyroxene (Holland and Powell, 2003), garnet, melt (White et al., 2014), biotite (Tajcmanova et al., 2009), plagioclase (Fuhrman and Lindsley,

1988), ilmenite (White et al., 2000). Magnetite, quartz, and aluminosilicates are considered pure phases. For the major element chemical analysis, the same slabs of the examined gneisses were used, which were previously used for thin-section preparation. The measured whole-rock composition of M-1A was normalised in mol%, are $SiO_2$ = 60.55, $Al_2O_3$ = 10.76, CaO = 2.26, FeO = 9.99, $K_2O$ = 2.22, MgO = 8.17, $Na_2O$ = 2.05, $TiO_2$ = 1.20, and LOI = 2.80. MnO content is low and hence neglected in pseudosection construction. Quartz is taken in excess as it is ubiquitous in all assemblages observed in pseudosection. Figure 8.10 shows the T-X ($H_2O$) pseudosection for sample M-1A (Grt-Bt gneiss) at 5 kbar. It shows that the observed mineral assemblage is stable at X($H_2O$) = 0.20 mol%-0.70 mol% at 5 kbar and 500–800°C. Ilmenite will disappear at higher X($H_2O$).

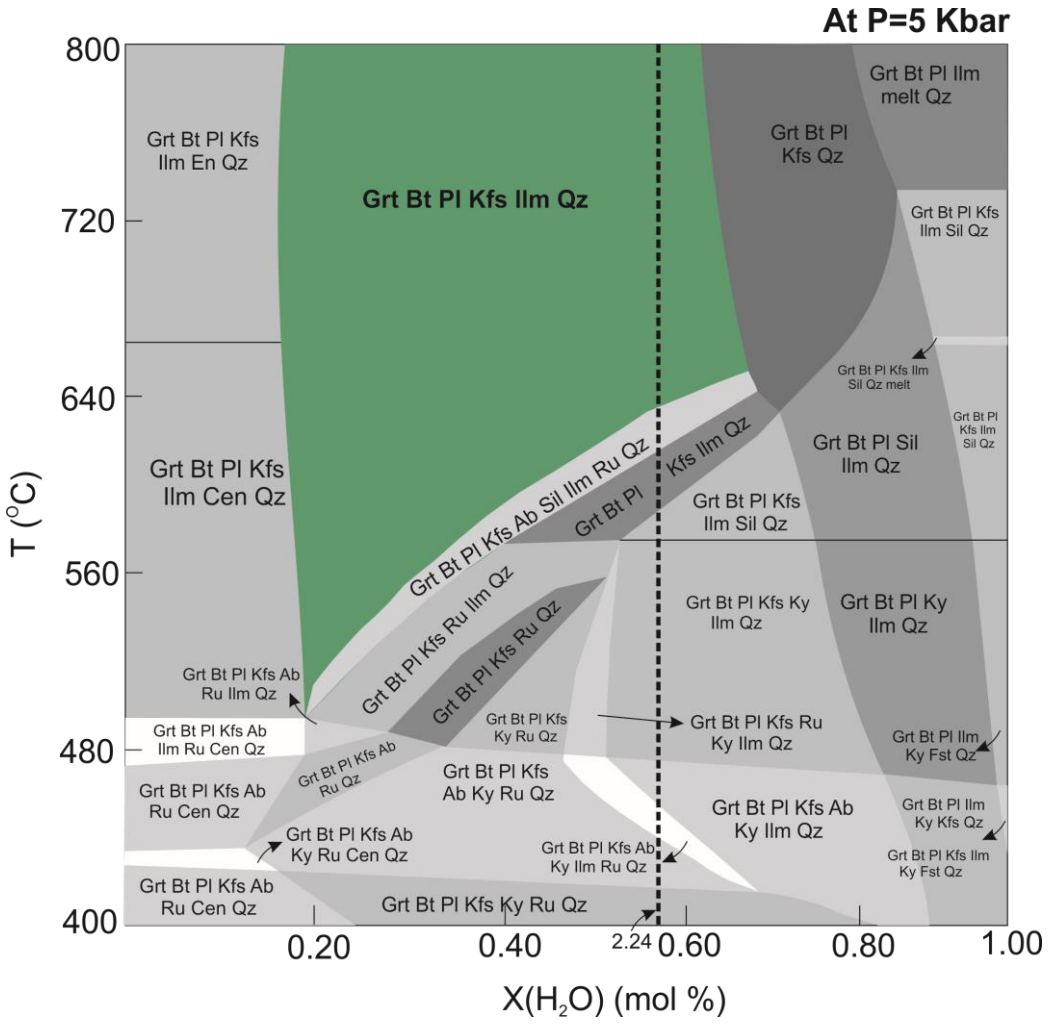


**Figure 8.10** T-X($H_2O$) diagrams showing calculated pseudosections of mineral assemblages in Grt-Bt gneiss (sample M-1A) at 5 kbar.

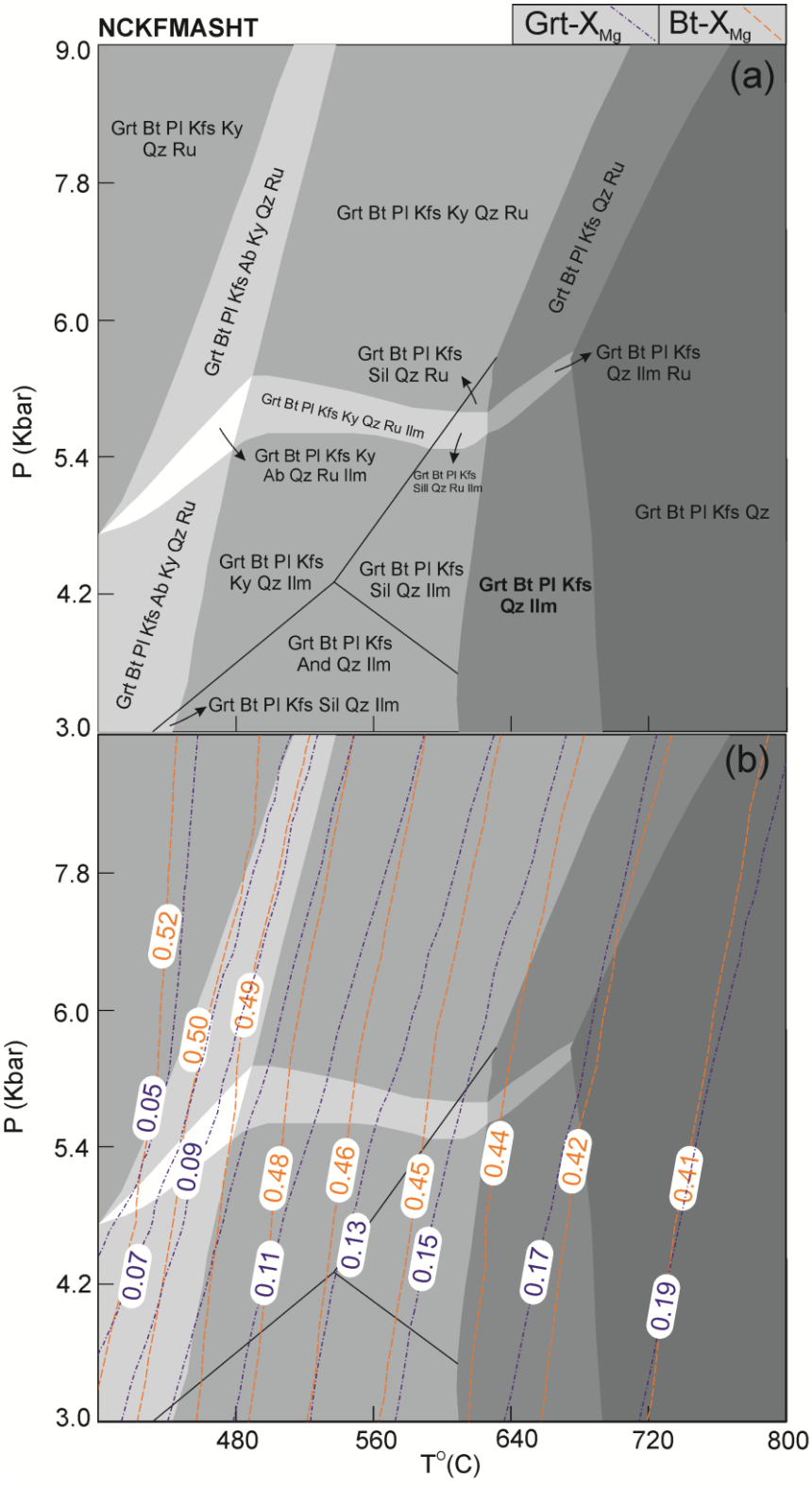


**Figure 8.11** (a) *P-T*pseudosection of mineral assemblage in Grt-Bt gneiss (sample M-1A) in the NCKFMASTH system (b) isopleths ($X_{Mg}$) of garnet and biotite contouring the *P-T* pseudosection.

We have constructed the *P-T* pseudosection for the same sample M-1A in the range of 3–9 kbar and 400–800ºC and it is represented in Figure 8.11a. The observed mineral assemblage

includes garnet, biotite, plagioclase, k-feldspar, ilmenite, and quartz. The stability field of the mineral assemblage is 3 kbar to 5.7 kbar and 600ºC to 700ºC. The upper-temperature limit of the assemblage is marked by the disappearance of ilmenite, whereas the lower temperature limit is marked by the appearance of sillimanite. The upper-pressure limit of the assemblage is marked by the appearance of rutile. The pseudosection is also contoured with the isopleths of $X_{Mg}$ garnet and $X_{Mg}$ biotite (Fig. 8.11b). Garnet isopleths show moderate slopes with $X_{Mg}$ content continuously increasing with increasing temperature, whereas the $X_{Mg}$ content of biotite constantly decreases with increasing temperature.

**8.B.4.3 Amphibolites**

Perple X ver.6.9.0 was used to create a pseudosection of the representative garnet-bearing (sample B-6) and garnet-absent (sample K-1, MM-1, BB-1) amphibolites (Connolly 2005, 2009). *P–T* pseudosections were calculated in the chemical system $Na_2O$-CaO-$K_2O$-FeO-MgO-$Al_2O_3$-$SiO_2$-$H_2O$-$TiO_2$-$O_2$ (NCKFMASHTO) for the B-6 and in the $Na_2O$-CaO-FeO-MgO-$Al_2O_3$-$SiO_2$-$H_2O$-$TiO_2$ (NCFMASHTO) system for the K-1, MM-1 and BB-1 which is reasonably compatible to the petrography of studied rocks. The activity composition models that are used in the pseudosection modelling are garnet, clinopyroxene, epidote, chlorite (Holland & Powell, 2003), amphibole (Diener et al. 2007), biotite (Tajcmanova et al. 2009), plagioclase (Fuhrman &Lindsley, 1988), ilmenite (White et al. 2000). For the major element chemical analysis, the same slabs of the examined amphibolites were used, which were previously used for thin-section preparation. B-6, K-1, MM-1 and BB-1 whole-rock compositions were normalized in mole percent. Because the contents of MnO and $P_2O_5$ are low, they are ignored in the construction of pseudosection of B-6, but $K_2O$ is also ignored in K-1, MM-1 and BB-1. Quartz is taken in excess as it is ubiquitous in all assemblages observed in pseudosection. T-X($H_2O$) and T-X($O_2$) pseudosections were used to calculate the $H_2O$ and $O_2$ content of both samples.

### (i) Garnet-bearing amphibolites

The assumed value of $H_2O$ and $O_2$ has been defined by the constructed T-X($H_2O$) and T-X($O_2$) pseudosection at a fixed pressure of 5.0 kbar for sample B-6 (Figs. 8.12a&b).

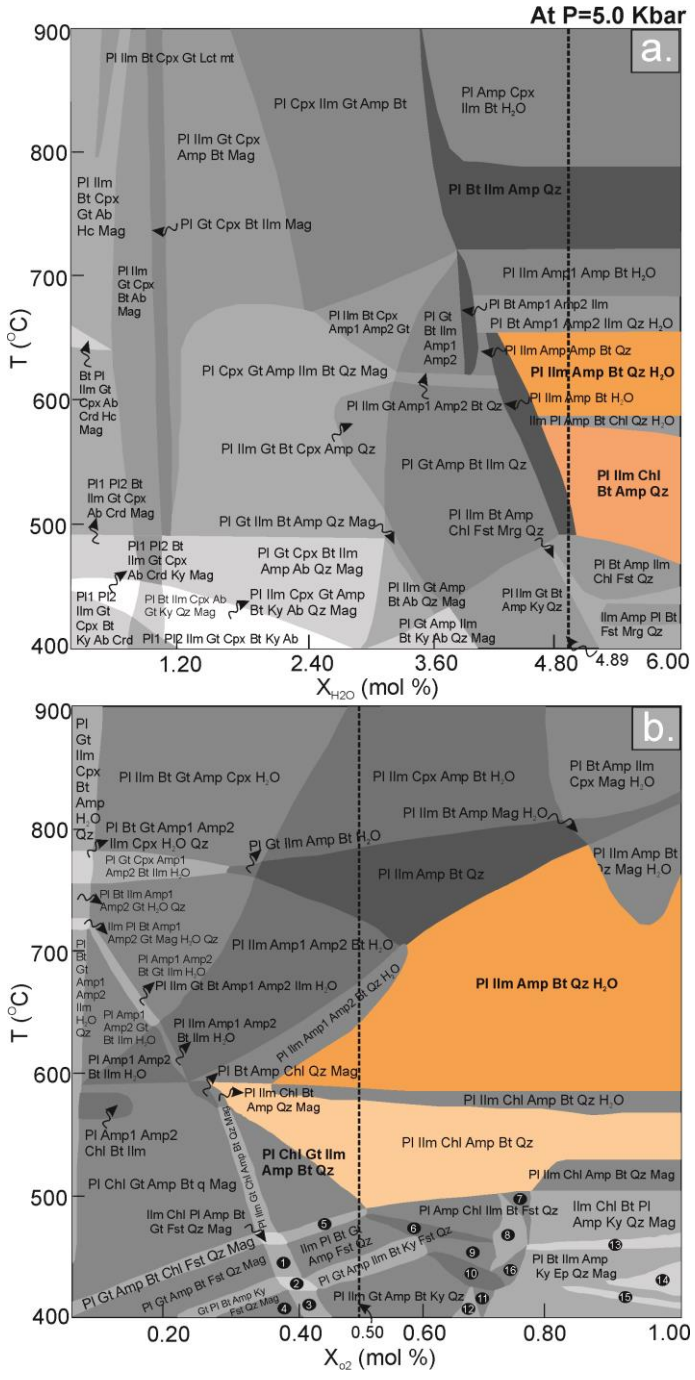


**Figure 8.12** (a) T-X($H_2O$) pseudosection calculated at fixed pressure 5.0 kbar, showing the effects of varying themolar proportions of bulk-rock $H_2O$ in garnet-bearing amphibolites (sample B-6). The black dashed line is showing the modelled composition of $H_2O$ (4.89 mol%). (b)T-X($O_2$) pseudosection calculated at fixed pressure 5.0kbar, showing the effects of varying the molar proportions of bulk-rock $O_2$ in same sample. The black dashed line is showing the modelled composition of $O_2$ (0.50 mol%).

The value of $H_2O$ was determined based on the variation of $H_2O$ in the bulk rock composition ranging from 0.0 to 6.0 mol%, whereas $O_2$ was calculated based on the variation of $O_2$ in the bulk rock composition ranging from 0.0 to 1.0 mol%. The meta-stable, pre-peak, and post-peak mineral assemblages are depicted in the T-X($H_2O$) diagram with the appropriate amount of X($H_2O$) = 4.89 mol%. Similarly, the T-X($O_2$) diagram reveals that a 0.50 mol% amount is appropriate, denoted by a large black dashed line. Therefore, 4.89 mol% of $H_2O$ and 0.50 mol% of $O_2$ are reliable amounts for further *P*–*T* pseudosection calculation.

The measured whole-rock composition of B-6 normalised in mol% are: $SiO_2$ = 49.88, $Al_2O_3$ = 11.50, CaO = 11.24, FeO = 12.38, $K_2O$ = 0.55, MgO = 7.20, $Na_2O$ = 1.35, $TiO_2$ = 0.60, $H_2O$ = 4.80 and $O_2$ = 0.49. The *P*–*T* pseudosection for sample B-6 was built in the *P*–*T* range 3–9 kbar and 400–900°C in the NCKFMASHTO system (Fig.8.13a). The mineral assemblages identified in the petrographic observations include garnet, amphibole, clinopyroxene, chlorite, plagioclase, biotite, quartz, and ilmenite. Garnet is temperature dependent, and as the temperature rises, it becomes more stable at higher pressures. Clinopyroxene is pressure-dependent and stable at higher temperatures. Amphibole is ubiquitous and stable in nearly all *P*–*T* fields, while plagioclase and biotite also predominate. The presence of amphibole, plagioclase, and biotite in petrographic thin sections supports their significant occurrence. Chlorite exists under medium pressure (4.0–6.6 kbar) and lower temperatures (400–550ºC) conditions as a meta-stable phase with amphibole and biotite. Pseudosection has validated three metamorphic stages for garnet-bearing assemblages, with the isopleth lines of garnet, amphibole, clinopyroxene, and biotites defining the appropriate *P*–*T* conditions of these metamorphic stages (Fig. 8.13b). The Amp-Chl-Bt-Pl-Qz-Ilm is a meta-stable mineral assemblage that may have formed before pre-peak metamorphism and is dominated by chlorite. This acquired phase is stable in the *P*–*T* range 3.2–6.2 kbar/420–550ºC, and amphibole and chlorite isopleths further narrow the *P*–*T* range to 4.35–4.1 kbar/515–475ºC.

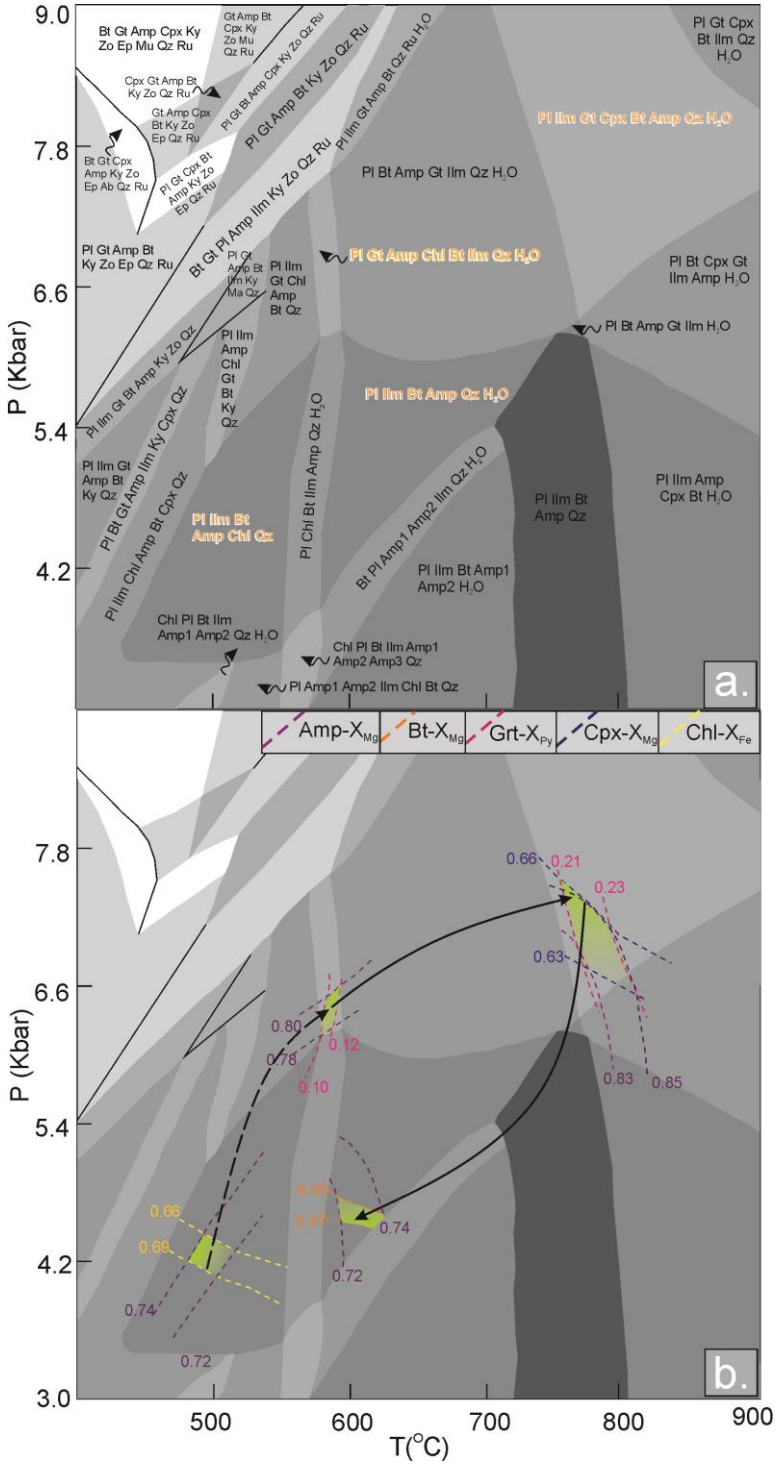


**Figure 8.13** (a) *P–T* pseudosection for garnet-bearing amphibolites (sample B-6), showing the metastable phase, pre-peak, peak and post-peak metamorphic condition. (b) Isopleths for amphibole, biotite, garnet, clinopyroxene, and chlorite are contoured in the *P–T* pseudosection.

The garnet appearance is recorded during the prograde phase, and the garnet becomes more stable as pressure and temperature increase. The pre-peak metamorphic assemblages are defined as Grt-Amp-Chl-Bt-Pl-Qz-Ilm-$H_2O$ and are stable in the *P–T* conditions of 6.2–7.5 kbar

and 570–595ºC. Amphibole and garnet isopleths defined the *P–T* conditions as 6.5–6.25 kbar and 590–580ºC. After the pre-peak metamorphic stage, chlorite is no longer stable. Following that, clinopyroxene appeared and became associated with garnet; this assemblage is regarded as the peak metamorphic stage for garnet-bearing amphibolite. The peak metamorphic assemblage is known as Grt-Amp-Cpx-Bt-Pl-Qz-Ilm-$H_2O$, occurring at higher *P–T* conditions. The *P–T* conditions for garnet-bearing amphibolite's peak metamorphic stage are 7.4–6.8 kbar/805–760 ºC using isopleth lines of amphibole, garnet, clinopyroxene, and biotite. After peak metamorphism, garnet and clinopyroxene are consumed to form amphibole; during retrograde metamorphism. The post-peak metamorphic assemblage has fewer mineral characteristics such as Amp-Bt-Pl-Qz- Ilm and is stable at a *P–T* range of 6.15–4.0 kbar and 750–580ºC. Amphibole and biotite isopleths reveal the *P–T* conditions of the post-peak metamorphism at 4.75–4.45 kbar/615–585ºC.

**(ii) Garnet-absent amphibolites**

**Sample K-1**

The T-X($H_2O$) and T-X($O_2$) pseudosections were constructed at 6.0 kbar pressure for sample K-1 (Figs. 8.14a&b). The value of $H_2O$ and $O_2$ used for pseudosection construction was determined based on the variation of $H_2O$ and $O_2$ in the bulk rock composition ranging from 0.0 to 6.0 mol%. The $H_2O$ value plotted on X-axis varies from 0.0 to 6.0 mol% in the T-X($H_2O$) diagram, and a black dashed line indicates the appropriate value of X($H_2O$) = 0.75(4.50 mol%). Similarly, the T-X($O_2$) diagram suggests that the appropriate amount of $O_2$ is 0.44 mol%, which is considered in the pseudosection construction.

The measured whole-rock composition of K-1 normalised in mol% are: $SiO_2$ = 49.73, $Al_2O_3$ = 11.71, CaO = 10.39, FeO = 10.73, MgO = 6.98, $Na_2O$ = 3.73, $TiO_2$ = 1.79, $H_2O$ = 4.50 and $O_2$ = 0.44. The *P–T* pseudosection was plotted for the garnet-absent amphibolites (sample K-1) under *P–T* ranges of 3–9 kbar and 400–900°C in the NCFMASHTO system (Fig. 8.15a).

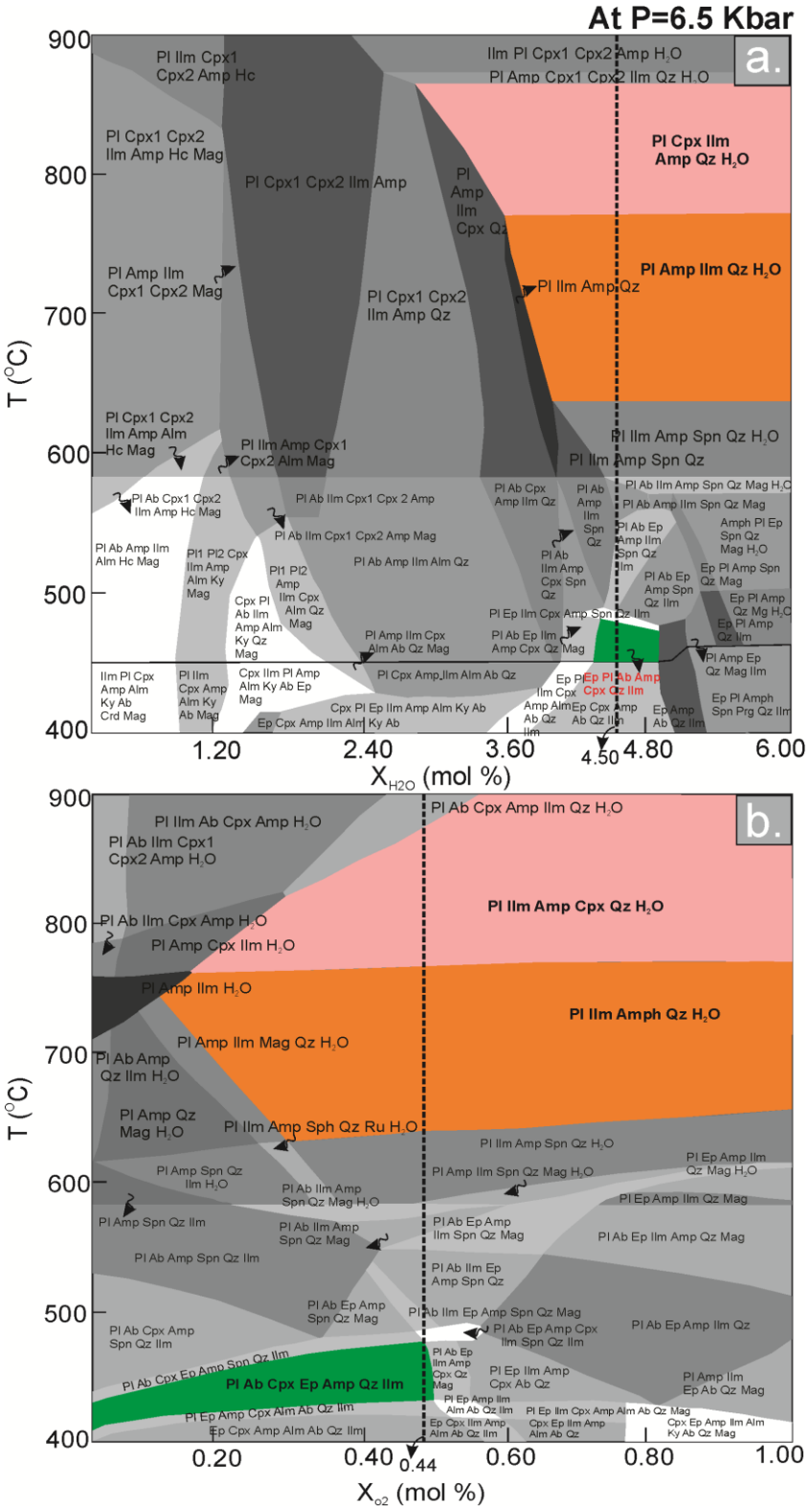


**Figure 8.14** (a) T-X($H_2O$) pseudosection calculated at fixed pressure 6.5 kbar, showing the effects of varying themolar proportions of bulk-rock $H_2O$ in garnet-absent amphibolites (sample K-1). The black dashed line is showing the modelled composition of $H_2O$ (4.50 mol%). (b)T-X($O_2$) pseudosection calculated at fixed pressure 6.5 kbar, showing the effects of varying the molar proportions of bulk-rock $O_2$ in same sample. The black dashed line is showing the modelled composition of $O_2$ (0.44 mol%).

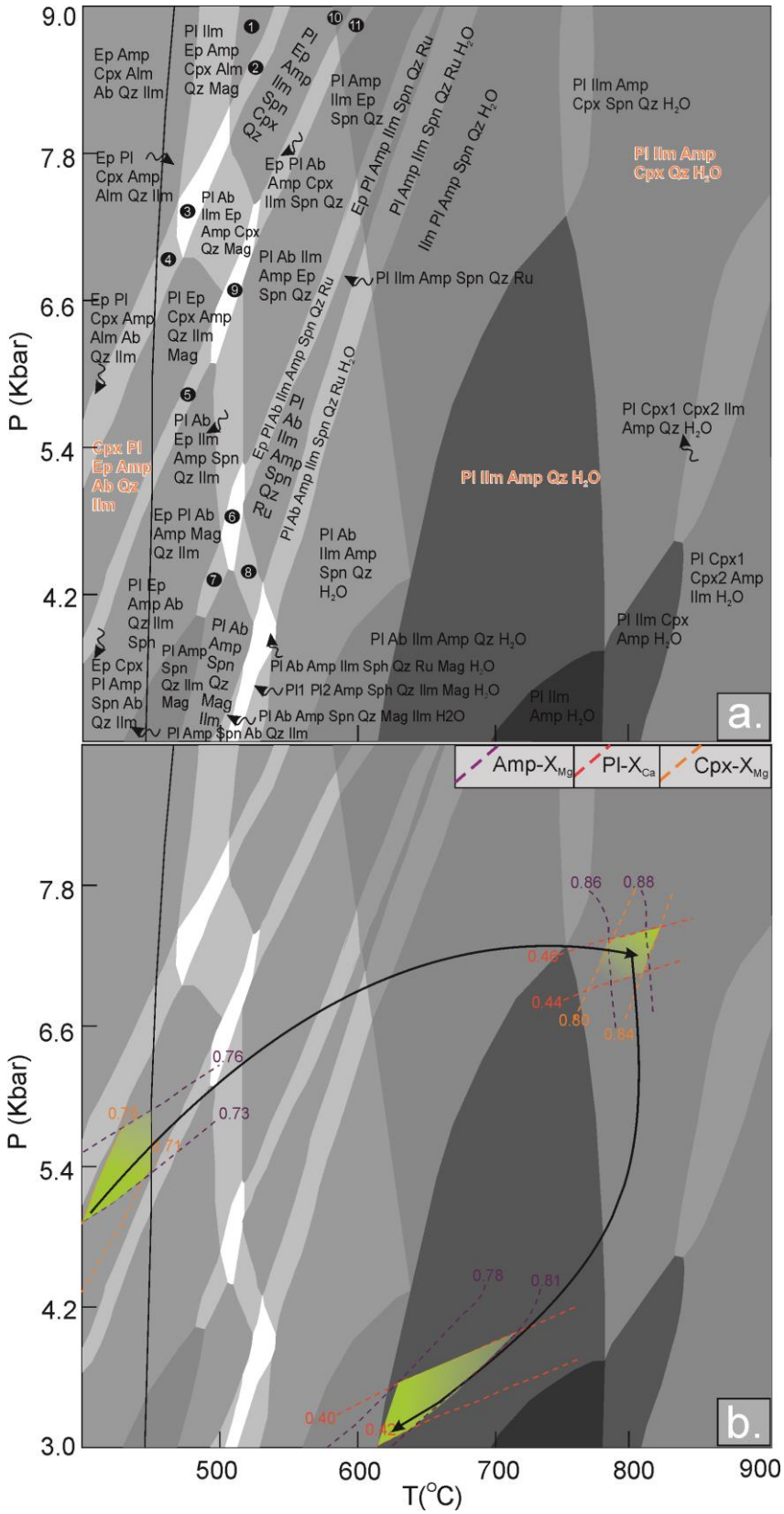


**Figure 8.15** (a) *P–T* pseudosection for garnet-absent amphibolites (sample K-1), showing the pre-peak, peak and post-peak metamorphic condition. (b) Isopleths for amphibole, plagioclase, and clinopyroxene are contoured in the *P–T* pseudosection.

The mineral assemblages identified in the petrographic observations include clinopyroxene, amphibole, epidote, plagioclase, quartz, and ilmenite. In the garnet-absent assemblage, three metamorphic stages have been identified. Amphibole and plagioclase are ubiquitous and stable in all *P–T* phases. Epidote is stable at lower temperatures (400–650ºC). The isopleths of amphibole, clinopyroxene, and plagioclase are delineated on the pseudosection to obtain the appropriate *P–T* conditions of the significant mineral assemblage metamorphism conditions of the significant mineral assemblage (Fig.8.15b). The mineral paragenesis Amp-Cpx-Ep-Pl-Qz-Ab-Ilm characterises the pre-peak metamorphism, acquiring the field in the *P–T* range 4.0–6.4 kbar/400–450ºC. Amphibole, clinopyroxene, and plagioclase isopleths narrow the *P–T* conditions of the pre-peak metamorphic stage to 5.8–5.0 kbar/400–450ºC. The peak metamorphic stage paragenesis is characterized by Cpx-Amp-Pl-Qz-Ilm-$H_2O$. In this case, epidote becomes unstable as the temperature rises and does not appear in the peak assemblage. Peak metamorphic assemblage is stable at 7.4–7.0 kbar/810–785ºC, which is demarcated by the isopleths of amphibole, clinopyroxene and plagioclase. Afterwards, clinopyroxene becomes unstable and consumed to form amphibole. The post-peak assemblage is denoted as Amp-Pl-Qz-Ilm-$H_2O$, and amphibole and plagioclase isopleths are used to define the *P–T* conditions of 4.0–3.1 kbar/710–620ºC.

**Sample MM-1**

T-X($H_2O$) diagram of sample MM-1 was built to specify the probable water content in stable constraints to distinct metamorphic stages and associated *P–T* requirements at 7.5 and 4.0 kbar, respectively. The $H_2O$ content is determined by the variation of $H_2O$ from 0.0 to 6.0 mol% in the bulk rock composition (Fig.8.16a&b). In the NCFMASHTO system, the appropriate mole ratios of oxides are normalized to 100%. As illustrated in Figures 8.16a&b, the epidote is unstable at lower $H_2O$ values before breaching the Ep entry line (yellow line). The solid red line indicates the appearance of $H_2O$ as the temperature increases. The pre-peak stage

mineral assemblage Ep-Amp-Cpx-Pl-Ilm-Ru-Qz is stable in X($H_2O$) values of 0.72–0.85 (long dashed black line). The observed mineral assemblage of peak stage, Amp-Cpx-Pl-Ilm-Ru-Qz, is stable for X($H_2O$) values 0.61–0.65, while the mineral assemblage of the post-peak stage Amp-Pl-Ilm-Ru-Qz does not appear at a higher pressure of 7.5 kbar, this is most likely due to the pressure value chosen being too high (Fig.8.16a).

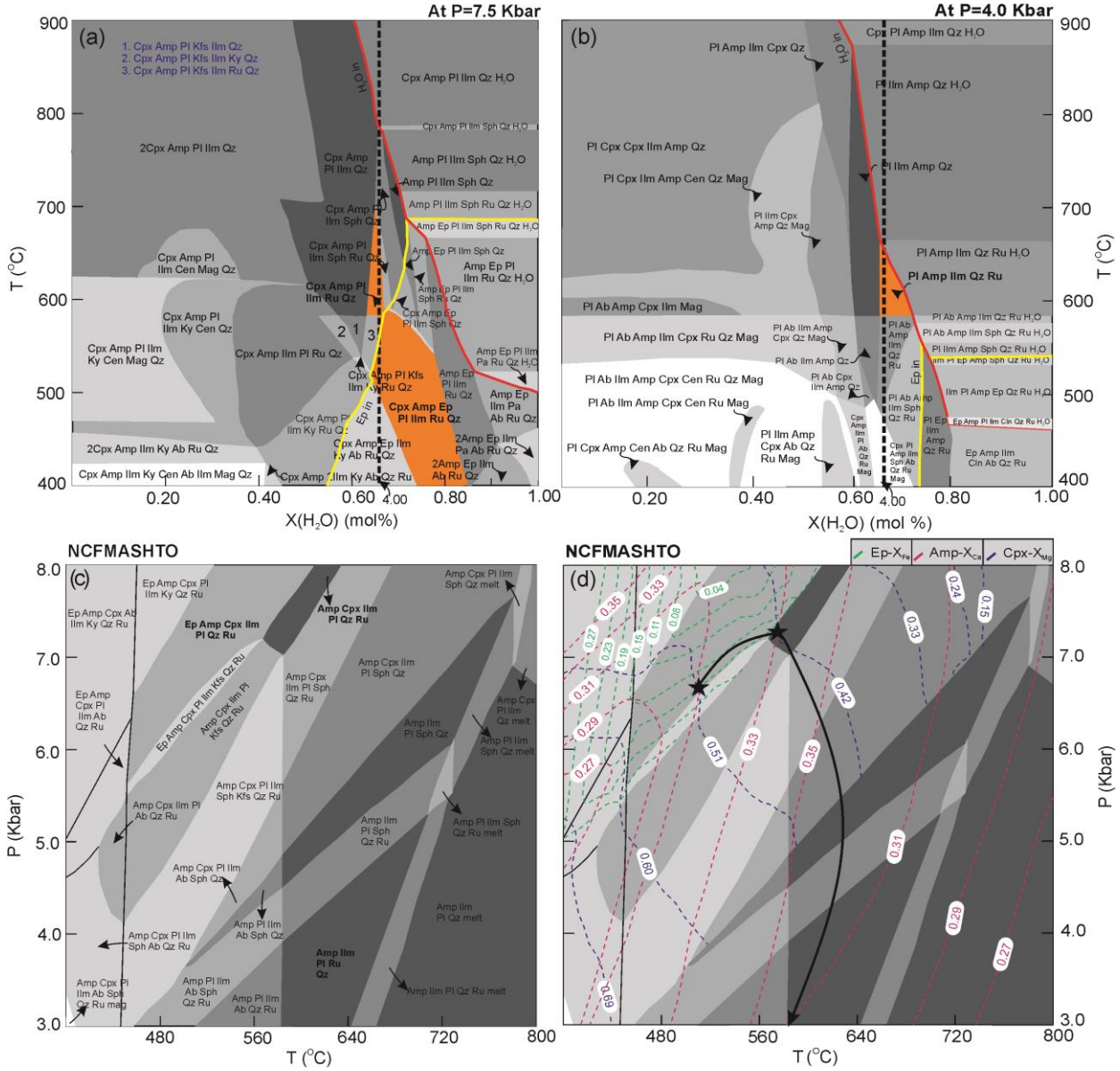


**Figure 8.16** (a) T-$X_{H2O}$ pseudosection at 7.5 Kbar, and (b) at 4.0 kbar, showing the effects of varying the molar proportions of bulk-rock $H_2O$ (in MM-1). The black dashed line is the modelled composition of $H_2O$ (4.00%). (c) *P-T* pseudosection showing pre-peak, peak and post-peak assemblages. (d) Isopleths$X_{Ca}$ of Amp, $X_{Mg}$Cpx and $X_{Fe}$ of Ep.

When the T-X($H_2O$) diagram is calculated at lower pressure values of 4.0 kbar, the post-peak stage mineral assemblage appears (Fig.8.16b). Hence, we chose an X($H_2O$) value of 4.00, which was calculated based on effective composition (Table 7) and then normalized to 100% by considering stable fields of mineral assemblages for pre-peak, peak and post-peak, which is marked by a black dash line and is also used to construct the *P–T* pseudosection diagram (Fig.8.16c&d). The mineral assemblages identified in the petrographic observations include clinopyroxene, amphibole, plagioclase, epidote, quartz, ilmenite, and rutile.

The measured whole-rock composition of MM-1 normalised in mol% are: $SiO_2$ = 50.42, $Al_2O_3$ = 9.16, CaO = 8.98, FeO = 9.45, MgO = 11.81, $Na_2O$ = 3.68, $TiO_2$ = 1.00, $H_2O$ = 4.00 and $O_2$ = 1.50. A *P–T* pseudosection for the sample MM-1 is constructed in the *P–T* range of 3–8 kbar and 400–800ºC in the NCFMASHTO system (Fig.8.16c). Clinopyroxene in the pseudosection is pressure-dependent and continuously increases with pressure, and it becomes stable under higher temperature conditions. Amphibole is ubiquitous and stable in approximately all *P–T* fields. Plagioclase also mostly appears in the pseudosection. The significant occurrence of amphibole and plagioclase is supported by the presence of amphibole and plagioclase in petrographic thin sections. The epidote is at higher pressures (4.5–8.0 kbar) and lower temperatures (400–600ºC). To acquire the appropriate *P–T* conditions for metamorphism of the significant mineral assemblage, the isopleths of amphibole, clinopyroxene, and epidote are delineated on the pseudosection (Fig.8.16d). During pre-peak metamorphism, clinopyroxene grains contain epidote, amphibole, plagioclase, ilmenite, and rutile, as represented by the mineral assemblage Ep-Amp-Cpx-Pl-Ilm-Ru-Qz, which is stable at a *P–T* range of 5.5–8.0 kbar and 450–600ºC. Amphibole, clinopyroxene, and epidote isopleths further narrow down the *P–T* conditions of the pre-peak metamorphic stage at 6.7 kbar and 510ºC. The mineral assemblage of Amp-Cpx-Pl-Ilm-Ru-Qz characterizes the peak metamorphic stage. The epidote becomes unstable with increasing temperatures. This assemblage is stable in a *P–T* range of 7.2–

8.0 kbar and 560–580ºC. Isopleths of amphibole and clinopyroxene defined the *P–T* conditions for the peak metamorphic stage at *P* = 7.3 kbar and *T* = 578ºC.

Later, the post-peak metamorphic stage is characterized by the mineral assemblage of Amp-Pl-Ilm-Ru-Qz, which acquires a Cpx-free field. Due to a lowering pressure, clinopyroxene is no longer stable at the post-peak metamorphic stage. This assemblage is stable under a *P–T* range of 3.0–5.0 kbar and 580–700ºC. Isopleths of amphibole reveal the *P–T* conditions of the post-peak metamorphic stage at *P* = > 3.0 kbar and *T* = > 585ºC.

**Sample BB-1**

The same process of computing $H_2O$ values was repeated for sample BB-1. Mole ratios of oxide are normalized to 100% in the NCFMASHTO system. At 6.5 and 4.0 kbar, a T-X($H_2O$) pseudosection was also displayed (Figs.8.17a&b). The epidote is unstable at lower $H_2O$ concentrations before breaching the Ep entry line, as seen in Figures 8.17a&b. As the temperature rises, the solid red line represents the emergence of $H_2O$. In X($H_2O$) values of 0.60–0.65, the pre-peak mineral assemblage Ep-Amp-Cpx-Pl-Ab-Ilm-Qz remains stable (long dashed black line). While the mineral assemblage of the peak stage Amp-Cpx-Pl-Ilm-Qz-$H_2O$ is stable for X($H_2O$) values of 0.61–1.00, the mineral assemblage of the post-peak stage Amp-Pl-Ilm-Qz-$H_2O$ does not appear in figure 8.17a at a higher pressure of 6.5 kbar, and this is most likely owing to the pressure value chosen being high. The post-peak and peak stage mineral assemblages became visible when the T-X($H_2O$) diagram was calculated at lower pressures of 4.0 kbar (Fig.8.17b). As a result, we chose an X($H_2O$) value of 4.00, which was calculated using effective composition and then normalized to 100% in the NCFMASHTO system by considering stable fields of mineral assemblages for pre-peak, peak and post-peak, which is marked by a black dash line and is also used to construct the *P–T* pseudosection diagram (Fig.8.17c&d).

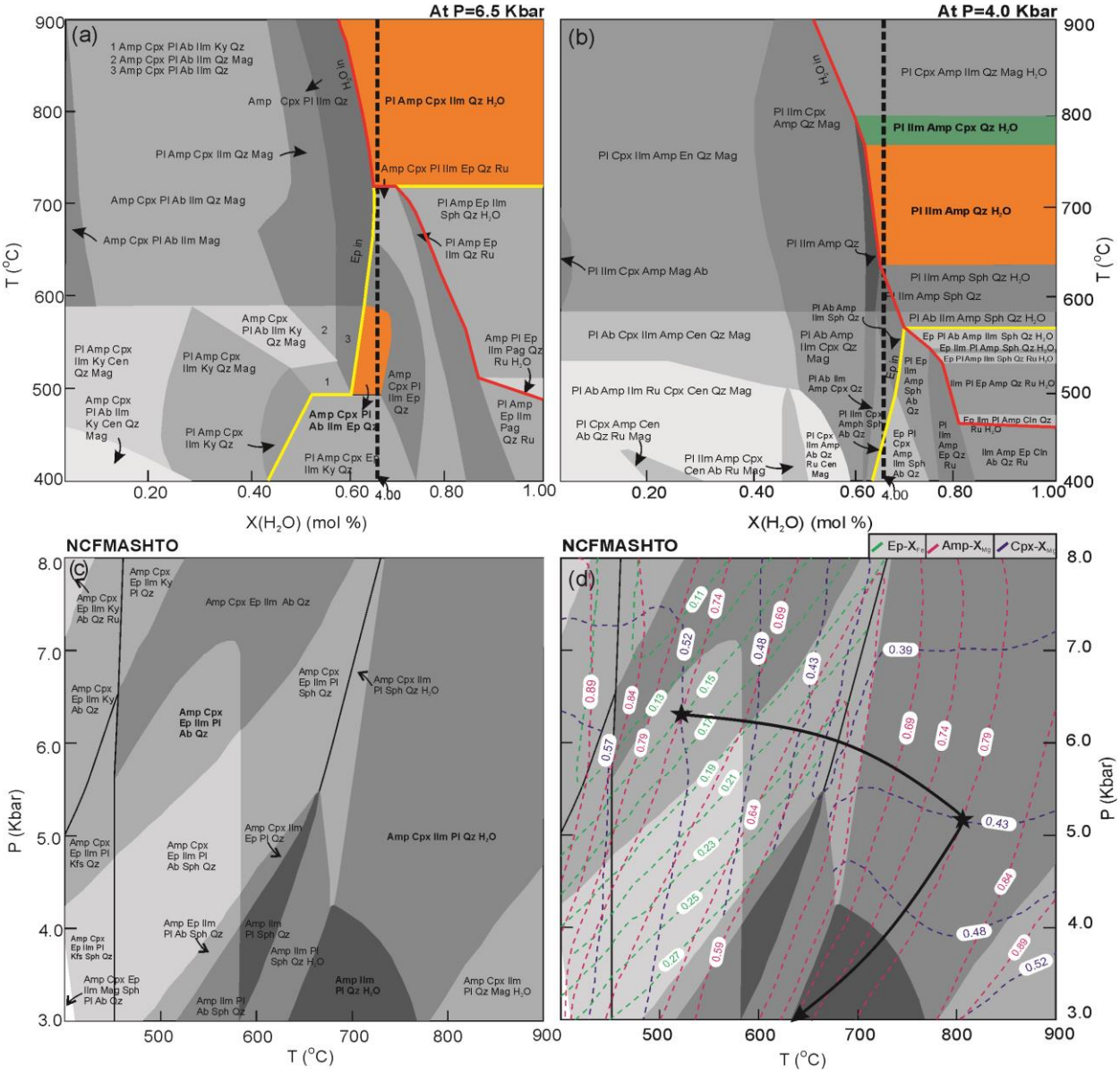


**Figure 8.17** (a) T-$X_{H2O}$pseudosection at 6.6 Kbar and (b) at 4.0 Kbar, showing the effects of varying the molar proportions of bulk-rock $H_2O$ in amphibolite (sample BB-1). The black dashed line is the modelled composition of $H_2O$ (4.00%). (c) *P-T*pseudosection (sample BB-1) of amphibolites showing pre-peak, peak and post-peak metamorphic assemblages in the NCFMASTHO system. (d) Isopleths$X_{Mg}$ of amphibole, $X_{Mg}$ of clinopyroxene and $X_{Fe}$ of epidote contouring *P-T* pseudosection.

The measured whole-rock composition of BB-1 normalised in mol% are: $SiO_2$ =50.78, $Al_2O_3$ = 9.58, CaO = 9.56, FeO = 9.49, MgO = 10.77, $Na_2O$ = 3.77, $TiO_2$ = 0.55, $H_2O$ = 4.00 and $O_2$ = 1.50.In the NCFMASHTO model system, a specific *P–T* pseudosection for the representative amphibolite sample (BB-1) has been generated in the *P–T* range of 3–8 kbar and 400–900ºC (Fig.8.17c). In the pseudosection, clinopyroxene shows a pressure-dependent

character and is stable at higher temperatures with other mineral phases such as amphibole, plagioclase, ilmenite, quartz, and $H_2O$. Amphibole is ubiquitous in all phases and is stable over a wide *P–T* range. Plagioclase is also found mostly in the pseudosection. Epidote can be found at high and low pressures (3.0–8.0 kbar) but only at much lower temperatures (> 680°C). The most common Ti-bearing phases are ilmenite and magnetite. This rock is devoid of rutile. The *P–T* pseudosection of the BB-1 sample revealed three stages of metamorphism. The first is the pre-peak metamorphic stage, which is characterized by epidote, amphibole, plagioclase, and ilmenite inclusions inside clinopyroxene grains. This stage produces the mineral assemblage Ep-Amp-Cpx-Pl-Ab-Ilm-Qz, stable in the pseudosection at *P–T* ranges of 4.8–7.0 kbar and 450–580°C. *P–T* conditions of the pre-peak metamorphic stage at P = 6.27 kbar and T = 520°C are further constrained by isopleths of amphibole, clinopyroxene, and epidote (Fig.8.17d). The peak metamorphic stage is defined by the mineral assemblage Amp-Cpx-Pl-Ilm-Qz-$H_2O$. With the rising temperature, the epidote becomes unstable, and $H_2O$ forms at a higher temperature. This assemblage obtains a field with a *P–T* of 3.0–8.0 kbar and a temperature of 680–900°C. The *P–T* conditions of the peak metamorphic stage at P = 5.2 kbar and T = 805°C are further narrowed by isopleths of amphibole and clinopyroxene. Finally, the mineral assemblage Amp-Pl-Ilm-Qz-$H_2O$ denotes the post-peak metamorphic stage. At the post-peak metamorphic stage, clinopyroxene is no longer stable. This assemblage acquires a field with a *P–T* of 3.0–4.2 kbar and a temperature of 620–780°C and is further defined as > 3.0 kbar and > 640°C by the isopleths of amphibole.